

## Measurement of the Heat Load Imposed on the Reactor Vessel Depending on the Debris Bed Under an IVR Condition

Joon-Soo Park, Hae-Kyun Park, Seong-II Baek and Bum-Jin Chung\*

Department of Nuclear Engineering, Kyung Hee University

#1732 Deogyong-daero, Giheung-gu, Yongin-si, Gyeonggi-do, 17104, Korea

\*Corresponding author: bjchung@khu.ac.kr

### 1. Introduction

In a severe accident condition, particulate debris generated by thermal shock and the dense debris may remain at the bottom of the oxide pool without completely melting after the relocation process of the molten corium [1–4]. Then, the debris bed formed and the geometrical condition of the oxide pool was changed, which may affect natural convection heat transfer of the oxide pool. However, only a few studies [1, 3] were performed regarding the in-vessel debris bed. We measured the variations of local heat flux distribution and comparative analyses were performed between with and without debris bed conditions with a few different bed heights.

### 2. Theoretical background

#### 2.1 Phenomena on oxide pool with in-vessel debris bed

Figure 1 shows the simulated severe accident sequence for APR1400 using MELCOR 2.1. The particulate debris was generated by thermal shock as shown in Fig. 1(d) [3]. Then, the molten corium and particulate debris deposited on the core supporting structure. The core supporting structure collapsed due to the decay heat. Then, the molten corium and particulate debris relocated to the lower head. The molten corium was stratified into a two-layer molten pool consisting of an upper light metal layer and a lower oxide pool by the density difference. The remaining debris, which had not completely melted, deposited at the bottom of the oxide pool and formed the in-vessel debris bed, as shown in Fig. 1(m). Formation of the in-vessel debris bed varies the geometric configuration of the oxide pool and it may act as an obstacle to the natural convective flow in the oxide pool. Hence, the heat load imposed on the reactor vessel could be affected.

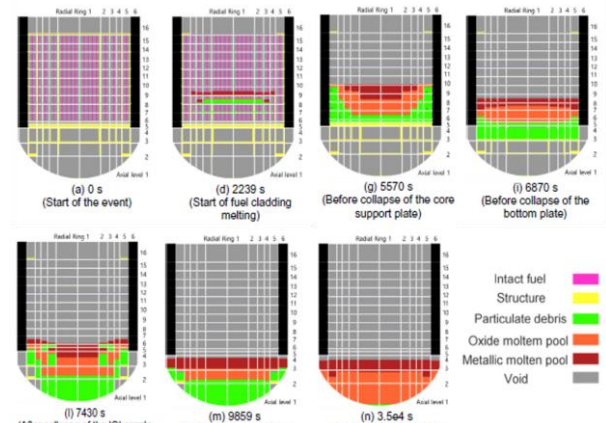


Fig. 1. In-vessel debris bed formation at the lower head (Reproduced from [3]).

### 3. Experimental setup

#### 3.1 Experimental methodology

Heat and mass transfer systems are analogous. This means that the governing equations of two systems are mathematically the same. Thus, the heat transfer problems can be solved by the mass transfer experiments [5].

The limiting current technique, a method of measurement, is used by the mass transfer system and developed by several researchers [6–8], and this methodology is now well-established [9–11].

By using the mass transfer system, we could achieve high  $Ra_H$  with compact test rigs, ideally isothermal cooling condition and uniform heat generation.

Our research group has been investigating the IVR problems simulating the various molten pool configurations such as 2- and 3-layer employing 2D and 3D test rigs using the experimental methodology. The detailed experimental methodology is described in our previous papers [9–11].

In the present work, the experimental method was applied to simulate heat transfer to the vessel, with and without in-vessel debris bed formation.

#### 3.2 Phenomenon modeling

To simulate the natural convection in the oxide pool under the in-vessel debris bed formed condition, we assumed that the outer vessel wall is maintained as

isothermal condition due to the ERVC and the temperature difference between inner and outer vessel wall was neglected to simplify modeling. Through these assumptions, the oxide pool boundary was simulated by an isothermal wall.

The reference height of the debris bed,  $H_{Bed}$ , was estimated as 0.093 m. The code calculation results in existing study and geometrical parameters of the lower head for APR1400 were employed to estimate the reference  $H_{Bed}$  [12, 13].

The particulate debris was simulated with identical diameter spheres. The diameter of the particulate debris was determined to be 0.004 m to avoid the influence of capillary force [14]. The porosity of the debris bed was 0.40–0.41, which was within a realistic range according to the TMI-2 investigation [4].

According to the simulation result using MELCOR [3], the debris melting sequence was not fast. Hence, we neglected the heat generation from the debris and simulate the in-vessel debris bed as adiabatic.

Table I lists the test matrix. The  $H_{Bed}$  was extended as 0.025–0.100 m based on reference  $H_{Bed}$ .

Table I: Test matrix

Debris bed formation	$H_{Bed}$ (m)	$Ra'_H$	$Pr$
Without debris bed	0	$1.22 \times 10^{15}$	2014
With debris bed	0.025	$1.14 \times 10^{15}$	
	0.050	$1.10 \times 10^{15}$	
	0.075	$1.07 \times 10^{15}$	
	0.100	$1.01 \times 10^{15}$	

Figure 2 presents the photographs of the Mass Transfer Experimental Rig for a 2D oxide pool with Debris Bed (MasTER-OP2(DB)), which radius is 0.168 m. The width is 0.0668 m, whose is enough to neglect the effect of the side wall [15]. The copper cathodes were located along the inner surface. To check the symmetry and horizontality of test rigs, halves of the inner surfaces consisted of a single electrode and the other halves consisted of piecewise electrodes for the local currents measurement. The curved surface consisted of twelve piecewise electrodes, and eight along the uppermost surface. To simulate the internal heat source, copper anodes were attached to both sides. Copper sulfate-sulfuric acid ( $\text{CuSO}_4\text{-H}_2\text{SO}_4$ ) solution was used as a working fluid.

The polystyrene spheres were used to simulate particulate debris. Its density is  $960 \text{ kg/m}^3$ , which is lighter than the working fluid, then the particulate debris could attach to the curved surface in an inverted test rig arrangement. The particulate debris was fixed using a permeable grid, which was electrically insulating. The cathode surface did not contact the grid to avoid current measurement problems.

Figure 3 presents the experimental circuit. Because the natural convective flow towards the bottom of the test rig is formed in heat transfer, anode could simulate as a cold wall in mass transfer. But, the current is not measured in anode [8]. Therefore, we performed the experiments using the inverted test rig arrangement against the gravity direction and simulated the same natural convective flow.

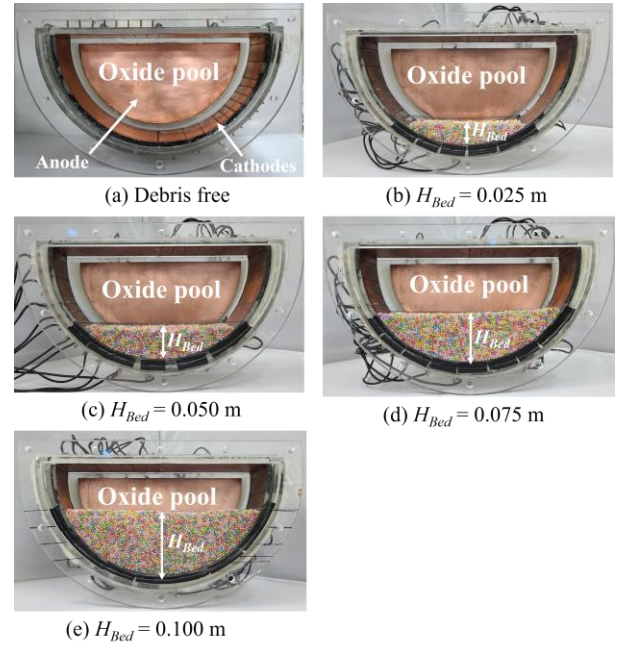


Fig. 2. Test rigs.

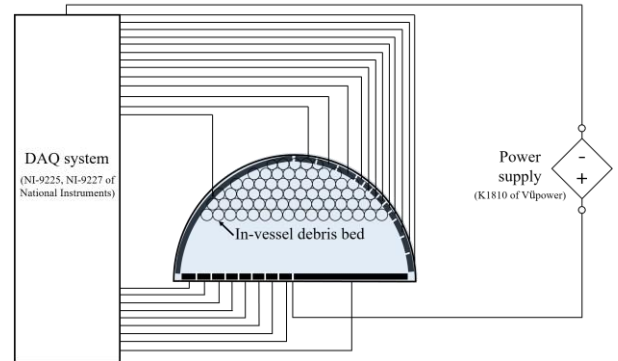


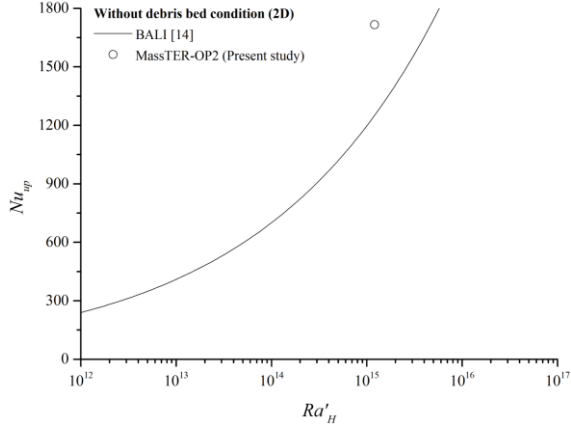
Fig. 3. Test circuit and inverted arrangement of test rig.

## 4. Results and discussion

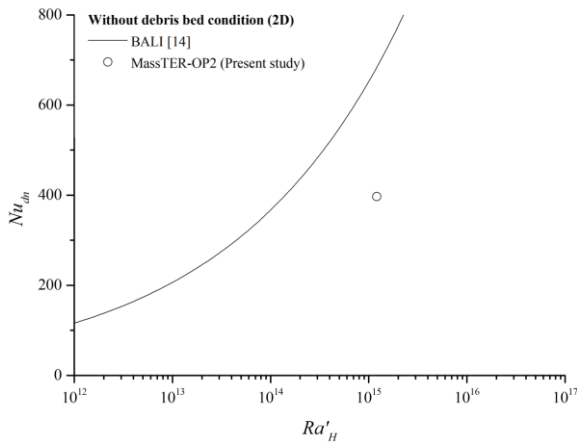
### 4.1 Comparison of the mean $Nu$ with existing study

Figure 4 compares our present result for the without debris bed condition with the correlation obtained from the BALI experiment [16]. For the without debris bed condition,  $Nu_{up}$  was 37% higher and  $Nu_{dn}$  was 42% lower than the BALI correlation. The discrepancies were associated with the large  $Pr$  of our mass transfer system as discussed in our previous works [9–11]. Due to the large  $Pr$ , a very thin thermal boundary layer was

created Thus, the rising plume efficiently conveyed hot fluid to the uppermost surface. However, the total mean  $Nu$ , the summation of  $Nu_{up}$  and  $Nu_{dn}$ , was 9% greater than BALI correlation.



(a) Mean  $Nu_{up}$  of the uppermost surface



(b) Mean  $Nu_{dn}$  of the curved surface

Fig. 4. Comparison of the Mean  $Nu$  with the existing study.

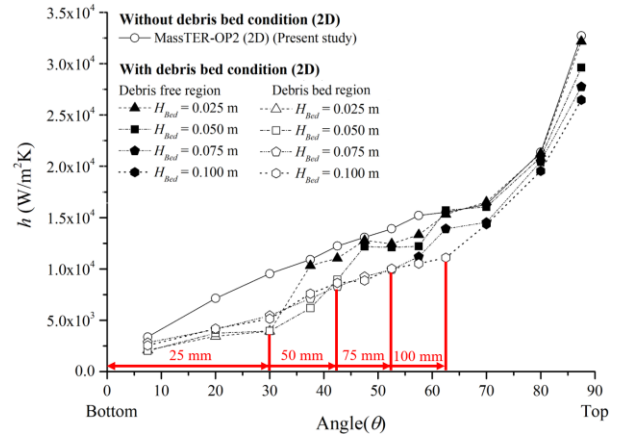
#### 4.2 Influence of the bed height on local heat transfer

Figure 5(a) presents the local heat transfer coefficients ( $h_{locS}$ ) measured along the curved surface for with and without debris bed condition. For without debris bed condition, the  $h_{locS}$  drastically dropped at the area covered by the debris compared to the debris free region. It was because of the reduction of the driving force due to the in-vessel debris bed. The debris bed acted as an obstacle to the natural convective flow. The descending flows along the curved surface were blocked and scattered by the debris bed. Once the descending flows passed the porous debris bed, the flows were scattered to various directions. Then, the flow rate reaching to the bottom of the curved surface was decreased. Hence, the height inducing the buoyancy was decreased, so that the driving force was reduced.

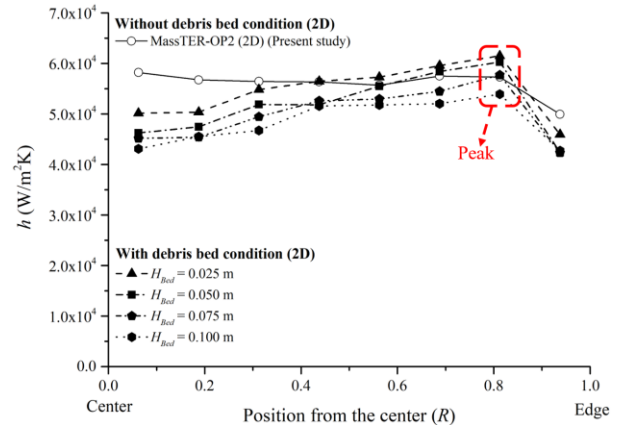
Figure 5(b) shows the  $h_{locS}$  measured at the uppermost surface. For the without debris bed condition, the  $h_{locS}$

had a peak at the center due to the rising plume, which conveyed the hot fluid from the bottom of the curved surface. Meanwhile, the  $h_{locS}$  decreased at the center in with debris bed condition. When the rising plume passed through the debris bed, the friction loss and flow dispersion occurred. For this reason, the plume was weakened before it reached the center of the uppermost surface and the  $h_{locS}$  decreased. The  $h_{locS}$  gradually increased from center to just before the edge for with debris bed condition. It seems to be occurred because of the dispersed plume due to the debris bed. The dispersed plume rose to the uppermost surface. As the dispersed plume generated at a higher point of the curved surface, the plume was less cooled. Hence, the  $h_{locS}$  showed a peak just before the edge for the debris bed condition, it was because the temperature difference between the plume and the uppermost surface increased. The dramatic decrease of the  $h_{locS}$  at the edge was induced due to the stagnant flow formed at the edge of the uppermost surface.

The local heat transfers at the uppermost surface, where the particulate debris did not contact, was impaired according to the increase of  $H_{Bed}$ . It seems to be induced by reduction of the driving force.



(a)  $h_{locS}$  of the curved surface



(b)  $h_{locS}$  of the uppermost surface

Fig. 5. Comparison of  $h_{locS}$  according to the bed height.

## 5. Conclusion

The natural convection heat transfers of the oxide pool when the debris bed was formed was simulated. We investigated the debris bed influence on the heat load imposed on reactor vessel under an IVR condition. The range of  $Ra'_H$  was  $\sim 10^{15}$ .

When the debris bed was formed in the oxide pool, the driving force of the natural convective flow was reduced because it acted as an obstacle to the flow. Therefore, the heat transfers at the uppermost and curved surface were impaired. This trend was enhanced with the increasing height of the debris bed.

Actually the expected configuration of debris bed was cone-like shape, not flat top. To consider this limitation, we will be performed further study, which changing configurations of the debris bed

## ACKNOWLEDGEMENT

This study was sponsored by the Ministry of Science and ICT (MSIT) and was supported by nuclear Research & Development program grant funded by the National Research Foundation (NRF) (Grant codes 2020M2D2A1A02065563).

This work was supported by the Korea Institute of Energy Technology Evaluation and Planning (KETEP) grant funded by the Korea government (MOTIE) (20214000000070)

## REFERENCES

- [1] Y. Jin, W. Xu, X. Liu and X. Cheng, In- and ex-vessel coupled analysis of IVR-ERVC phenomenon for large scale PWR, *Annals of Nuclear Energy*, Vol. 80, pp. 322–337, 2015.
- [2] W. Ma, Y. Yuan and B.R. Sehgal, In-vessel melt retention of pressurized water reactors: Historical review and future research needs, *Engineering*, Vol. 2, pp. 103–111, 2016.
- [3] K.H. Lim, Y.J. Cho, S.W. Whang and H.S. Park, Evaluation of an IVR-ERVC strategy for a high power reactor using MELCOR 2.1, *Annals of Nuclear Energy*, Vol. 109, pp. 337–349, 2017.
- [4] D.H. Nguyen, F. Fichot and V. Topin, Investigation of the structure of debris beds formed fuel rods fragmentation, *Nuclear Engineering and Design*, Vol. 31, pp. 96–107, 2017.
- [5] A. Bejan, *Convection Heat Transfer*, Third ed, New York: John Wiley & Sons, INC, pp. 96-97, 173-179, 197-200, 512-516, 2006.
- [6] V. G. Levich, *Physicochemical Hydrodynamics*, Prentice-Hall, Englewood Cliffs, New Jersey, 1962.
- [7] E. J. Fenech, C. W. Tobias, Mass transfer by free convection at horizontal electrodes, *Electrochimica Acta*, Vol. 2, pp. 311-325, 1960.
- [8] Y. Konishi, Y. Nakamura, Y. Fukunaka, K. Tsukada and K. Hanasaki, Anodic Dissolution Phenomena Accompanying Supersaturation of Copper Sulfate Along a Vertical Plane Copper Anode, *Electrochimica Acta*, Vol. 48, pp. 2615–2624, 2003.
- [9] H. K. Park, S. H. Kim and B. J. Chung, Natural Convection of Melted Core at the Bottom of Nuclear Reactor Vessel in a Severe Accident, *International Journal of Energy Research*, Vol. 42, pp. 303–313, 2018.
- [10] J. W. Bae and B. J. Chung, Comparison of 2-D and 3-D IVR experiments for oxide layer in the three-layer configuration, *Nuclear Engineering and Technology*, Vol. 52, pp. 2499–2510, 2020.
- [11] J.S. Park, H.K. Park and B.J. Chung, Influence of crust formation on the heat load to a reactor vessel under an in-vessel retention condition, *Annals of Nuclear Energy*, Vol. 166, 108813, 2022.
- [12] R.J. Park and S.W. Hong, Effect of SAMG entry condition on operator action time for severe accident mitigation, *Nuclear Engineering and Design*, Vol. 241, pp. 1807–1812, 2011.
- [13] R.J. Park, K.S., Ha and H.Y. Kim, Detailed evaluation of natural circulation mass flow rate in the annular gap between the outer reactor vessel wall and insulation under IVR-ERVC, *Annals of Nuclear Energy*, Vol. 89, pp. 50–55, 2016.
- [14] L. Barleon, K. Thomauske and H. Werle, Cooling of debris beds, *Nuclear Technology*, Vol 65, pp. 67–86, 1984.
- [15] T.N. Dinh, R.R. Nourgaliev and B.R. Sehgal, On heat transfer characteristics of real and simulant melt pool experiments, *Nuclear Engineering and Design*, Vol. 169, pp. 151–164, 1997.
- [16] J.M. Bonnet, J.M. Seiler, Thermal hydraulic phenomena in corium pools: the BALI experiment, in: 7th international Conference on Nuclear Engineering, Tokyo, Japan, April 19–23, 1999.